FR 8002102

INIS

Ninth Texas Symposium on relativistics astrophysics.
Munich, RFA, December 14 - 18, 1978.
CEA - CONF 4690

COS-B OBSERVATION OF THE MILKY WAY IN HIGH-ENERGY GAMMA RAYS

H.A. Mayer-Hasselwander, K. Bennett,
G.F. Bignami, R. Buccheri, N. D'Amico,
W. Hermsen, G. Kanbach, F. Lebrun,
G.G. Lichti, J.L. Masnou, J.A. Paul,
K. Pinkau, L. Scarsi, B.N. Swanenburg,
R.D. Wills

COS-B OBSERVATION OF THE MILKY WAY IN HIGH-ENERGY GAMMA RAYS

H.A. Mayer-Hasselwander[4], K. Bennett[6], G.F. Bignami[2], R. Buccheri[4], N. D'Amico[3], W. Hermsen[1], G. Kanbach[4], F. Lebrun[5], G.G. Lichti[6], J.L. Masnou[5], J.A. Paul[5], K. Pinkau[4], L. Scarsi[3], B.N. Swanenburg[1], R.D. Wills[6]

[1]Cosmic Ray Working Group, Huygens Laboratory, Leiden, The Netherlands

[2]Laboratorio di Fisica Cosmica e Tecnologie Relative del C.N.R., Università di Milano, Italy

[3]Laboratorio di Fisica Cosmica e Tecnologie Relative del C.N.R., Università di Palermo, Italy

[4]Max-Planck-Institut für extraterrestrische Physik, Garching bei München, Federal Republic of Germany

[5]Service d'Electronique Physique, Centre d'Etudes Nucléaires de Saclay, France

[6]Space Science Department of the European Space Agency, ESTEC, Noordwijk, The Netherlands

1. Introduction

The Caravane Collaboration's gamma-ray astronomy experiment aboard ESA's satellite COS-B has been recording celestial gamma rays in the energy range from about 50 MeV to several GeV since August 1975. The experiment features a spark chamber for gamma-ray event identification and determination of incidence direction, a CsI energy spectrometer for the measurement of gamma-ray energy and an assembly of particle counters for event selection and triggering. A description of the experiment is given by Bignami et al.[1] and its characteristic parameters are given by Scarsi et al.[2].

Most of the 37 observations, of typically one month duration, which were performed up to the end of 1978, were devoted to the study of the galactic disc. The 20 observations listed in Table 1 have been

used for the present analysis. These observations cover the whole range of galactic longitude, thus making it possible to present here the first complete detailed gamma-ray survey of the Milky Way with greatly improved statistical accuracy and significantly better energy measurement than in the previous survey by the SAS-2 mission.[3]

The present work concentrates on the spatial aspects of the gamma radiation, including localised sources, while the detailed analysis of spectral properties[18] and possible time variations are not sufficiently advanced to be reported here.

2. Method of Analysis

All the gamma-ray events used have been selected according to criteria which were defined to give a good compromise between sensitive area, field of view, angular resolution, energy measurement and background rejection. The spark-chamber data were analysed by an automatic pattern-recognition programme which identified likely gamma-ray events. These were subsequently visually scanned in order to remove background and improve the accuracy of the direction determination. Figure 1 shows the basic experiment characteristics for paraxial incidence and the particular selection criteria adopted in the present analysis. The energy bands used in the presentation are also indicated. The band boundaries were chosen to give sufficient statistical accuracy (similar numbers of gamma rays were recorded in each range) and to allow the assumption of a constant angular resolution (point-spread function) in each of the three intervals. The field of view was limited to 18° half-cone

in order to minimise possible systematic errors in measuring gamma rays at large angles of incidence with respect to the experiment axis without significant loss of overall sensitivity.

Special investigations were conducted on individual observation-period data sets in order to assess and correct for variations of experiment sensitivity caused by aging of the spark-chamber gas and by occasional experiment malfunctions. Such corrections, of a magnitude between 5 and 20%, were applied to 10 of the observations used.

In total, about 64000 gamma ray events were finally accepted and processed in order to derive contour maps and profiles of the gamma-ray intensity. The data were grouped in $0.5^{o} \times 0.5^{o}$ bins so as not to lose fine structure in regions of high intensity. The resulting small average number of events per bin necessitated a careful smoothing to make a clear overall presentation possible. The smoothing procedure developed and used was required to represent as perfectly as possible a data surface in the sky map whose structure is limited by the extension of the experiment point-spread function which, in this case, is strongly energy dependent, i.e. it should not suppress the sharpest physically possible peaks. On the other hand, in order to have a smoothing effect, the procedure should not reproduce significantly narrower peaks, which evidently can only be due to statistical fluctuations.

It has been found that the use of 2-dimensional polynomials across such a large matrix of data points leads either to flattening or to oscillation. If small regions are treated individually, the use of spline functions also results in undesired flattening of real

structures. The following satisfactory method has been developed. A data matrix A, describing the sky map within each energy band is produced. The data show statistical fluctuations. Each element of A is smoothed by the following process: a small (e.g. 9 x 9 element) matrix B, the local matrix, centred on the element of A, is extracted. This local matrix B is then approximated by a 2-dimensional Legendre polynomial. The smoothed value in the central element of B is then transferred into the new matrix C, which finally replaces A. The most appropriate degree of the polynomials and the size of the local matrix have been determined by testing within each energy range. It was found that best results were achieved with 3rd-degree polynomials in all cases. The local matrix sizes used for the different energy ranges are given in Table 2. In order to obtain a map representing the total range of energies, the smoothed maps prepared in the 3 energy ranges were summed.

The flux from a sky bin k of angular size ω_k (sr), from which N_k gamma-ray events were recorded, is given by

$$F_k = \frac{1}{T\ \omega_k} \sum_{i=1,N_k} \frac{1}{\epsilon(E_i)\eta\ (\vartheta_i, E_i)} \quad \text{photon cm}^{-2}\text{s}^{-1}\text{sr}^{-1}$$

where E_i is the energy of event i

ϑ_i is its incidence angle relative to the experiment axis

T(s) is the observation time

$\epsilon(E)$ (cm^2) is the experiment's effective sensitive area for paraxial incidence (see Fig. 1)

$\eta(\vartheta, E)$ describes the decrease of effective sensitive area with incidence angle.

Since, as a consequence of the spectrum of the galactic gamma rays, the spatial characteristics of a photon-flux map over the total energy range from 70 to 5000 MeV are dominated by the low energy quanta which are measured with least accuracy in angular resolution, a sky map has been generated showing the parameter 'on-axis counts' defined by the equation

$$G_k = \frac{1}{T\ \varpi_k} \sum_{i=1,N_k} \frac{1}{\eta(\vec{s},E)} \quad \text{count } s^{-1}sr^{-1}$$

This gives directly the number of gamma-ray events which would have been recorded in the bin k if the experiment had been pointed there, observing it 'on-axis'.

In the presented figures a background has been subtracted or is indicated. This background has been determined from two observations at galactic latitudes around 70 degrees and 45 degrees. It consists mainly of instrumental background with remaining galactic radiation and a small extragalactic component.

3. Galactic Gamma Ray Emission between 70 MeV and 5 GeV

Figure 2 shows a map of the galactic gamma-ray emission measured by COS-B, together with longitude and latitude profiles. For the map, a combination of grey scale and contour lines has been chosen to represent the smoothed data matrix, produced according to the method described in Chapter 2.

The applied smoothing can be considered to be minimal in the sense that only fluctuations of angular scale smaller than the point-

spread function are suppressed. On the other hand, not all individual features in the smoothed map are statistically significant. In order to allow a one page representation of the galaxy, a limited number of contour lines has been used. As a consequence, some significant fine structure is suppressed. Additional insight to the data is provided by the longitude and latitude profiles, which also give quantitative information on the statistical uncertainties. The background, as indicated by the shaded band in the longitude profile, has been subtracted.

In Figure 3, longitude profiles in three energy ranges are shown, indicating that more structure becomes visible at higher energies, due to better angular resolution. This fine structure has been separately investigated by cross-correlating the data with the point-spread function of the instrument. This analysis led to the recognition of a number of statistically significant enhancements which are consistent with the expected point source appearance, but which may also be due to extended features up to an angular size of two degrees, depending on intensities and energies.[4]

The preliminary result of this analysis is presented in Figure 4 and Table 3. The small flux range (about a decade) of the resolved sources[4,21] is one of the characteristics of present experiments in gamma ray astronomy. This is so because the sources are seen with limited angular resolution against a high background of unresolved galactic emission. In fact, further granularity in the emission of the disc is suggested by the data.

Latitude profiles were prepared in the highest energy range and were used to determine the intrinsic thickness of emissivity by

folding gaussian trial functions representing the intrinsic thickness of emissivity with the appropriate point-spread function. Only the inner part of the measured and simulated profiles were used for the fit. Examples illustrating this procedure are shown in Figure 5 together with variation of the unfolded angular thickness of the emitting region along the galactic disc.

The upper example indicates a narrow component, which is well fitted, and an asymmetric wide component which is disregarded by the method. In the lower example, only one component is present and is fitted.

4. Correlation between the Observed Gamma Ray Emission and Galactic Features

The combination of Figures 2-5 gives the overall appearance of the galactic gamma radiation with its resolved (sources) and unresolved components. When trying to understand it in terms of possible correlations with the structures in our Galaxy, one has first to bear in mind that gamma-ray astronomy provides a projected picture of the sky, with no independent method for measuring the distance of the emitting features. The only exceptions to this are the identified galactic sources, the four pulsars,[17] for which distance estimates are available from radio measurements.

The two components in the disc emission, seen in the upper profiles of Figure 5, and noted first by Fichtel et al.[3] in the SAS-2 data, can be related to features at different distances in the Galaxy by assuming a constant thickness for the gamma-ray disc.

This gives the first clear indication that the data refer both to parts of the Galaxy at 4 to 6 kpc distance and to much more local regions at < 1 kpc if this disc is about 200 pc thick. As for the distant features, their galactic longitude dependence is important and will be seen to relate them to large scale structures of the Galaxy; whereas the local component is found to be less dependent on longitude and can be well correlated to the local matter distribution. This correlation stems from the asymmetry of the latitude dependence of the wide components, with a broad excess at positive latitudes in the central region and the corresponding (less clearly defined) excess at negative latitudes in the anticentre.

Together with a possible evidence for a localised source in the Ophiucus dark cloud complex (see Table 3), this can be considered a good indication of gamma-ray emission from such local structures as Gould's Belt, at distances varying up to 450 pc from the Sun. If such an identification, as already suggested by Fichtel et al.,[3] is accepted, then a production mechanism based on the interactions of cosmic rays, both protons and electrons, with nearby interstellar clouds, is in this case clearly at work (refs. 5,6,7). Without performing a correlation with the individual clouds (apart from the Ophiucus case), it is important to note that, assuming a production rate of gamma rays of $\sim 2 - 3 \times 10^{-25}$ photon (> 100 MeV) sec^{-1} per equivalent H atom (see refs. 8,9,19), the approximately correct flux of gamma rays can be reproduced with a mass distribution for Gould's Belt as given by Lindblad,[10] Rossano,[11] and references therein. Whether this is

true for the particular case of the Ophiucus complex is still open.

Considering now the gamma-ray emission from more distant features, one should try to suppress from the map of Figure 2 the effects of the local structures described above, plus the obvious identified sources including the brightest gamma-ray emitter in the sky, the local PSR 0833-45, which coincides by chance with the galactic disc. What remains is a mixture of resolved and unresolved emission especially bright for $55^{\circ} \geq \ell \geq 285^{\circ}$. This general enhancement is well established in gamma-ray astronomy[3,12] and indicates that most of the emission of gamma radiation takes place in the inner Galaxy.

The correlation of the gamma-ray emission with the large scale features of the Galaxy can be based on the following:

(1) The small, but significant, latitude displacement of the peak emission visible in the profiles of Figure 2, as well as in the source distribution given in Figure 4, corresponds well to the "hat brim" effect seen in HI (21 cm line) and considered to be a tracer of the large scale warping of the plane.

(2) As far as the longitude variation of the intensity is concerned, the "galactic hole" at $\ell \sim 60^{\circ}$, an empty interarm region, is present in the gamma ray profile. Also apparent is the difference in the shape of the longitude profile in the central region, smoother from 0° to 50° and rougher from 300° to 360°. Finally, the emission from the Cassiopeia-Perseus-Taurus ($\ell \sim 110^{\circ} - 170^{\circ}$) region is enhanced with

respect to that in the Monoceros-Puppis-Vela region ($\ell \sim 210^{\circ} - 250^{\circ}$) which is kown as another particularly empty region of the disc.

No detailed correlation will be attempted here with particular features, nor with any model of the galactic spiral structure, as has been done by a number of authors on the basis of the SAS-2 data, which also contained similar indications (ref. 13 and references therein , refs. 14,20). This is not done because such modelling implies assumptions on the production scenarios which are not unique. Moreover, assumptions are needed on whether the large scale emission is related to diffuse "elementary" processes (gas and cosmic rays) or is more granular and clumpy in nature, i.e. possibly due to the sum of unresolved sources. The results presented here leave open the problem of the relative contribution of "source" and "diffuse" processes. Certainly, sources like those already recognised in the COS-B data do contribute to the general galactic emission. The possible amount of this contribution has been discussed by Bignami et al.[15] and Protheroe et al.[16].

In conclusion, it is important to note that the data presented here refer to galactic structures on the scale of both several kpc and several hundred pc, and that they <u>are</u> related to the structure of the Galaxy as it is known from radio data. Moreover, we have evidence of at least two types of gamma-ray emitter in the Galaxy, the pulsars[17] and the local clouds in Gould's Belt. No final conclusion can yet be reached on the nature of the large scale emission because of the present experimental impossibility of unravelling its small scale intrinsic geometry.

We thank P. Caraveo and A. Pollock for valuable discussions.

G.G.L. acknowledges receipt of an ESA fellowship.

References

1. Bignami, G.F., G. Boella, J.J. Burger, P. Keirle, H.A. Mayer-Hasselwander, J.A. Paul, E. Pfeffermann, L. Scarsi, B.N. Swanenburg, B.G. Taylor, W. Voges & R.D. Wills. 1975. Space Sci. Instrum. 1:245.

2. Scarsi, L., K. Bennett, G.F. Bignami, G. Boella, R. Buccheri, W. Hermsen, L. Koch, H.A. Mayer-Hasselwander, J.A. Paul, E. Pfeffermann, R. Stiglitz, B.N. Swanenburg, B.G. Taylor & R.D. Wills. 1977. Proc. 12th ESLAB Symposium, Frascati, ESA SP 124:3.

3. Fichtel, C.E., R.C. Hartman, D.A. Kniffen, D.J. Thompson, G.F. Bignami, H. Ögelman, M.E. Özel & T. Tümer. 1975. Astrophys. J. 198:163.

4. Hermsen, W., K. Bennett, G.F. Bignami, G. Boella, R. Buccheri, J.C. Higdon, G. Kanbach, G.G. Lichti, J.L. Masnou, H.A. Mayer-Hasselwander, J.A. Paul, L. Scarsi, B.N. Swanenburg, B.G. Taylor & R.D. Wills. 1977. Nature 269:494.

5. Black. J.H. & G.G. Fazio. 1973. Astrophys. J. 185:L7.

6. Puget, J.L., C. Ryter, G. Serra & G.F. Bignami. 1976. Astron. Astrophys. 50:247.

7. Lebrun, F. & J.A. Paul. 1978. Astron. Astrophys. 65:187.

8. Cesarsky, C.J., J.A. Paul & P.G. Shukla. 1978. Astrophys. and Space Sci. 59:73.

9. Fichtel, C.E., G.A. Simpson & D.J. Thompson. 1978. Astrophys. J. 222:833.

10. Lindblad, P.O., K. Grope, A. Sandqvist & J. Schober. 1973. Astron. Astrophys. 24:309.

11. Rossano, G.S. 1978. Astron. J. 83:241.

12. Bennett, K., G.F. Bignami, R. Buccheri, W. Hermsen, G. Kanbach, F. Lebrun, H.A. Mayer-Hasselwander, J.A. Paul, G. Piccinotti, L. Scarsi, F. Soroka, B.N. Swanenburg & R.D. Wills. 1977. Proc. 12th ESLAB Symposium, Frascati, ESA SP 124:83.

13. Bignami, G.F., C.E. Fichtel, D.A. Kniffen & P.J. Thompson. 1975. Astrophys. J. 199:54.

14. Paul, J.A., M. Cassé & C.J. Cesarsky. 1976. Astrophys. J. 207:62.

15. Bignami, G.F., P. Caraveo & L. Maraschi. 1978. Astron. Astrophys. 67:149.

16. Protheroe, R.J., A.W. Strong, A.W. Wolfendale & P. Kiraly. 1979. Nature, in press.

17. Buccheri, R., K. Bennett, G.F. Bignami, N. D'Amico, W. Hermsen, D.J.H. Huizing, G. Kanbach, G.G. Lichti, J.L. Masnou, H.A. Mayer-Hasselwander, J.A. Paul, B. Sacco, B.N. Swanenburg & R.D. Wills. 1979. Astron. Astrophys., in press.

18. Paul, J.A., K. Bennett, G.F. Bignami, R. Buccheri, P. Caraveo, W. Hermsen, G. Kanbach, H.A. Mayer-Hasselwander, L. Scarsi, B.N. Swanenburg & R.D. Wills. 1978. Astron. Astrophys. 63:L31.

19. Strong, A.W., A.W. Wolfendale, K. Bennett & R.D. Wills. 1978. Mon.Not.R.ast.Soc. 182:751.

20. Stecker, F.W. 1977. Astrophys. J. 212:60.

21. Swanenburg, B.N. 1979. Gamma-Ray Sources: A Puzzle or a Piece of a Puzzle? In 'Stars and Stellar Systems'. Astrophysics and Space Science Library. Reidel. Dordrecht, in press.

Figure Captions

Figure 1 Characteristic parameters of the experiment for the data selection requirements applied in this analysis and for paraxial incidence of gamma rays. The angular resolution is indicated by the FWHM of the twodimensional point-spread function.

Figure 2 Presentation in galactic coordinates of the structure of the galactic gamma-ray emission as measured by COS-B. In the map the surface fitted to the data matrix is indicated by contour lines and a grey scale. The accepted field of view is indicated by dashed circles. The latitude profiles show the data points with errors and the fitted surface (full line). The longitude ranges over which the data are averaged are indicated by brackets. In these profiles and in the map a background is subtracted. In the longitude profile the data points with errors averaged over ± 5 degrees are shown. The full line indicates a cross-section through the fitted surface along the galactic equator. The background is indicated by the shaded area. The map and the profiles show the parameter 'on-axis' counts $\cdot s^{-1} \cdot sr^{-1}$.

Figure 3 Longitude profiles of 'on-axis' counts in three energy ranges. The full line indicates the fitted surface. The background is indicated.

Figure 4 The point sources as listed in Table 3 are shown together with a tentative spectral hardness indication. Complex regions, where resolution of sources is difficult, and pulsars are specifically indicated.

Figure 5 Two examples for latitude distributions ('on-axis' counts $\cdot$ s^{-1} $\cdot$ sr^{-1}) are given. Data points, fitted surface and simulated distributions are shown. At the bottom the thickness of the gaussian distributions (2σ), describing the unfolded intrinsic emissivity at varying galactic longitude, and their position in latitude are given.

TABLE 1

Observations Used in the Analysis

Observation	Pointing Direction ℓ (deg)	b (deg)	Epoch from	to
1	184.0	-6.1	1975 - 08-17	1975 - 09-17
2	5.2	0.0	09-17	10-20
3A	263.5	-3.3	10-20	11-08
3B	262.7	+5.5	11-08	11-28
4	73.9	+0.3	11-28	12-24
5	291.6	+0.2	12-24	1976 - 01-23
7	321.5	+0.3	1976 - 02-23	03-24
8	25.7	+1.5	03-24	04-24
9	44.9	-2.1	04-24	05-24
11	125.8	+1.1	06-24	07-24
13	352.1	+8.5	08-21	09-30
14	195.3	+4.3	09-30	11-02
16	101.0	-0.9	12-10	1977 - 01-17
17	155.4	0.0	1977 - 01-17	02-24
18	5.2	-1.0	02-24	03-07
19	219.5	0.0	03-07	04-14
21	243.3	-2.4	05-02	06-08
22	84.1	+0.5	06-08	07-15
24	345.3	-4.5	08-18	09-23
25	35.3	+0.3	09-23	11-01
26	60.0	+0.1	11-01	12-07
28	140.9	+0.1	1978 - 01-13	1978 - 02-22

TABLE 2

Local Matrix Sizes

Energy Range (MeV)	Matrix Size	
	elements	angular extent
70 - 150	15 x 15	7.5^{o} x 7.5^{o}
150 - 300	11 x 11	5.5^{o} x 5.5^{o}
300 - 5000	9 x 9	4.5^{o} x 4.5^{o}

TABLE 3

GAMMA-RAY SOURCES DETECTED BY COS-B (see notes below)

Galactic Coordinates l^{II}	b^{II}	Number of observations	Spectral class	Remarks
21.0	+1.0	1	Soft	PSR 1822-09
65.5	0.0	3	Hard	CG 64+0
75.0	0.0	1	x	CG 75+0
78.5	+1.5	1	x	CG 78+1
95.5	+4.5	2	Hard	-
106.0	+1.5	1	x	-
121.0	+3.5	1	Hard	CG 121+3
135.5	+1.5	2	Medium	CG 135+1
176.0	-7.0	1	Soft	CG 176-7
184.5	-5.5	2	Medium	CG 185-5, PSR 0531+21
189.0	+1.0	1	x	CG 189+1
195.5	+4.5	2	Hard	CG 195+4
219.0	-0.5	1	Medium	-
243.0	-2.5	1	Hard	PSR 0740+28
263.5	-2.5	5	Hard	CG 263-2, PSR 0833-45
270.0	-1.0	2	Soft	-
284.0	-1.0	1	Hard	-
288.5	-0.5	1	Medium	-
291.0	+65.0	1	Medium	CG 291+65, 3C273
295.5	+0.5	1	Medium	-
312.0	-1.5	1	x	CG 312-1
327.5	-0.5	1	x	CG 327-0
333.5	0.0	1	x	CG 333+0
353.0	+16.0	1	Hard	in Ophiucus Dark Cloud Complex

Notes

1. The information is preliminary; analysis continues.
2. Error circles for positions have radii between 0.5° and 2.0°.
3. With the exception of CG 263-2 source intensities (> 100 MeV) are within the range 0.2 to 1.0 times that of CG 185-5.
4. Spectral classification is based on the relative numbers of photons detected in the ranges 50 to 150 MeV and > 150 MeV.
5. The pulsar identifications are confirmed by timing phase analysis.
6. Sources marked x are located in complex regions where more detailed analysis is needed to provide information additional to that given in the first COS-B catalogue.

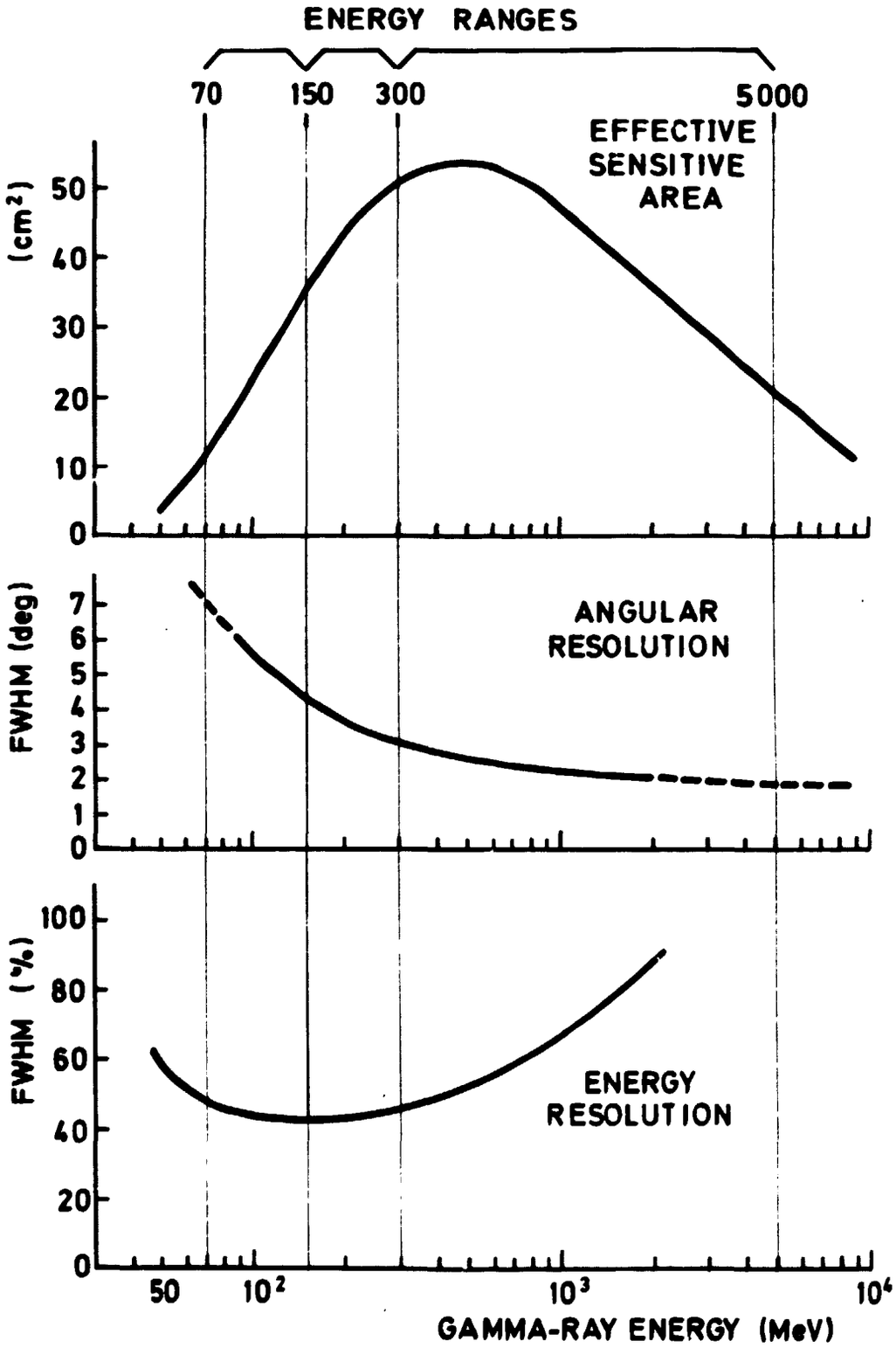
ENERGY RANGES
70
150
300
5000
EFFECTIVE SENSITIVE AREA
(cm²)
50
40
30
20
10
0
FWHM (deg)
7
6
5
4
3
2
1
0
ANGULAR RESOLUTION
FWHM (%)
100
80
60
40
20
0
ENERGY RESOLUTION
50
10²
10³
10⁴
GAMMA-RAY ENERGY (MeV)

Figure 1

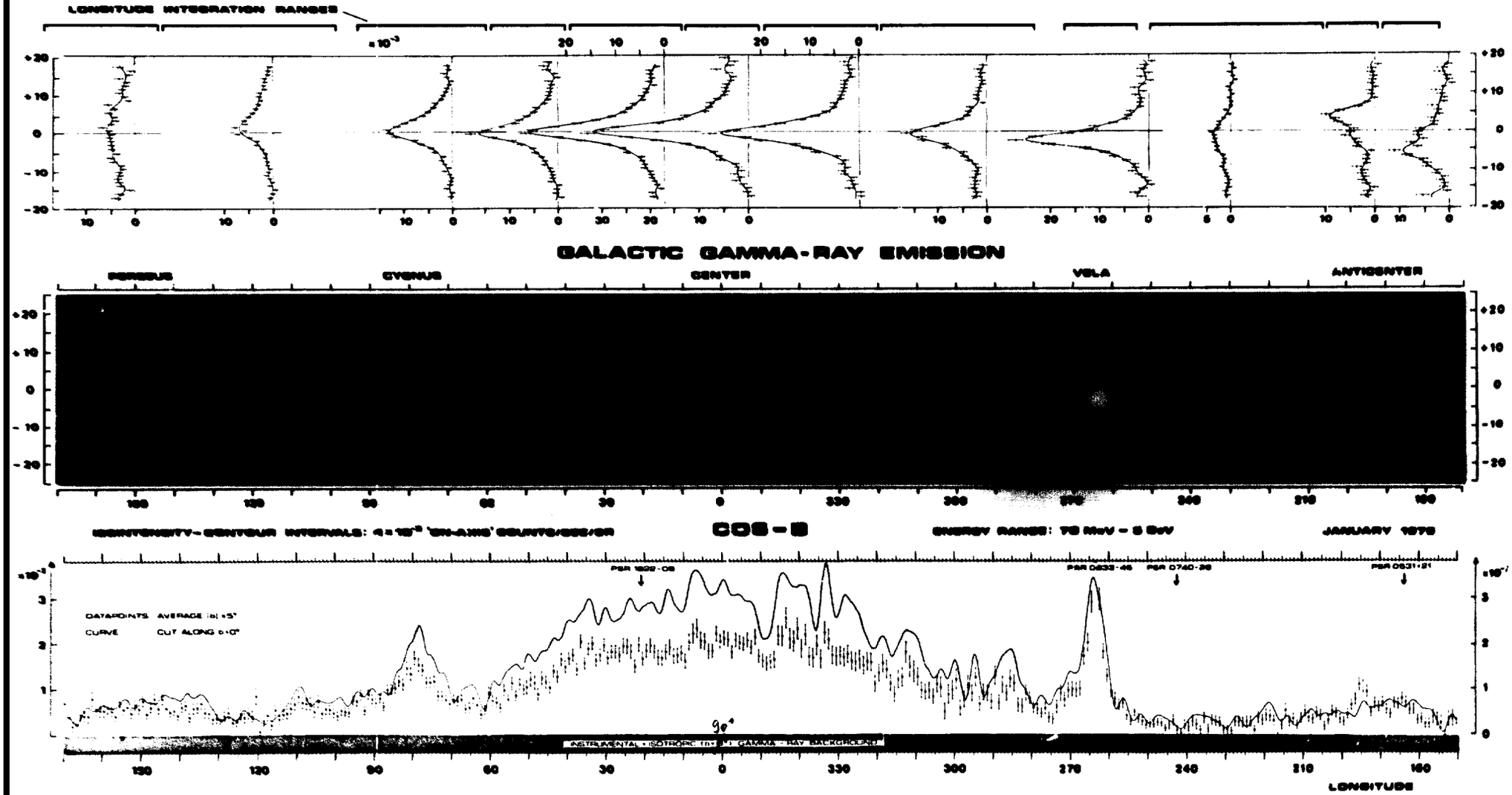
LONGITUDE INTEGRATION RANGES
GALACTIC GAMMA-RAY EMISSION
PERSEUS
CYGNUS
CENTER
VELA
ANTICENTER
COS-B
JANUARY 1975
DATAPOINTS AVERAGE (b) ±5°
CURVE CUT ALONG b=0°
PSR 1822-09
PSR 0833-45
PSR 0740-28
PSR 0631+21
INSTRUMENTAL + ISOTROPIC (n+i) GAMMA - RAY BACKGROUND
LONGITUDE

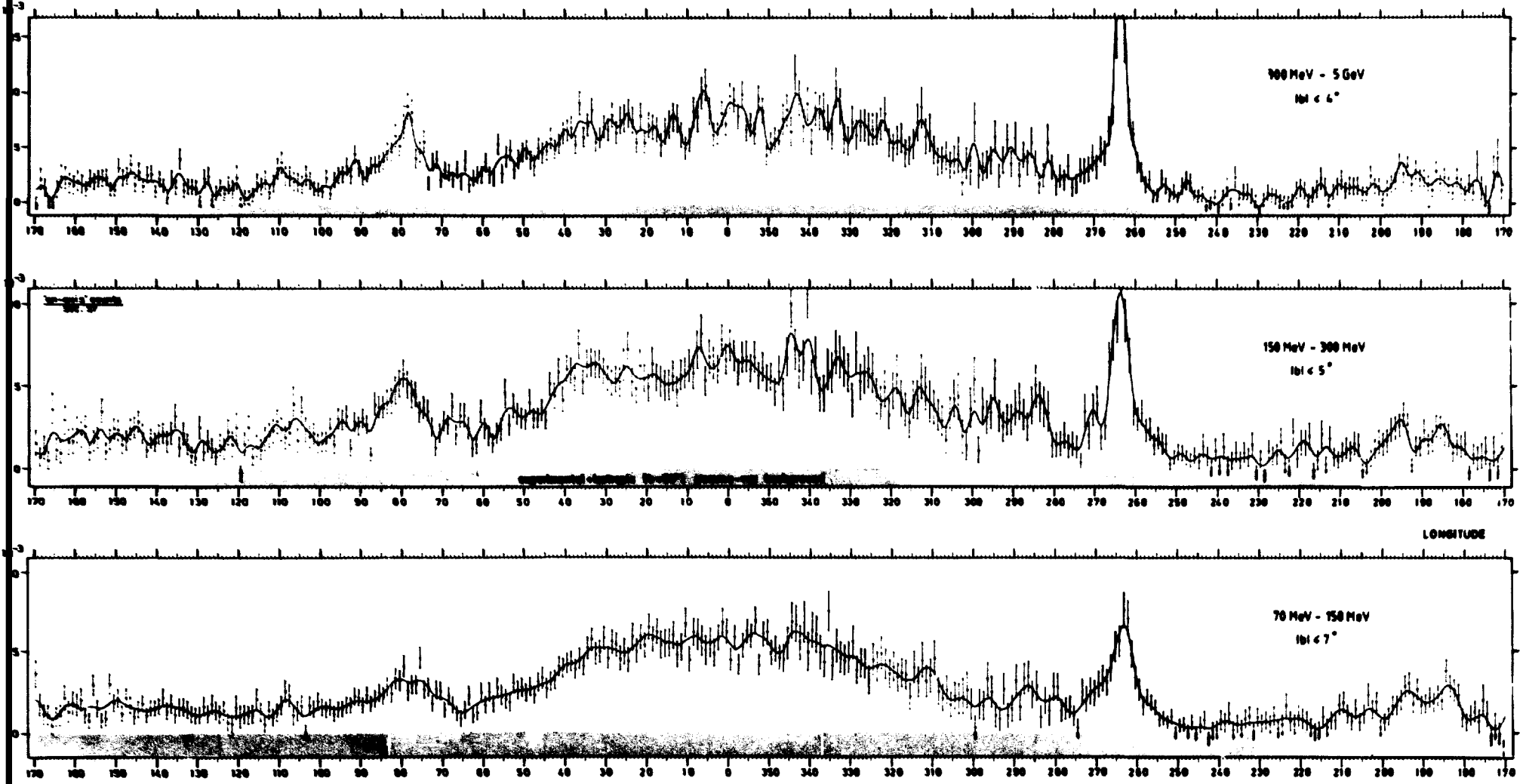
100 MeV - 5 GeV
|b| < 4°
150 MeV - 300 MeV
|b| < 5°
70 MeV - 150 MeV
|b| < 7°
LONGITUDE

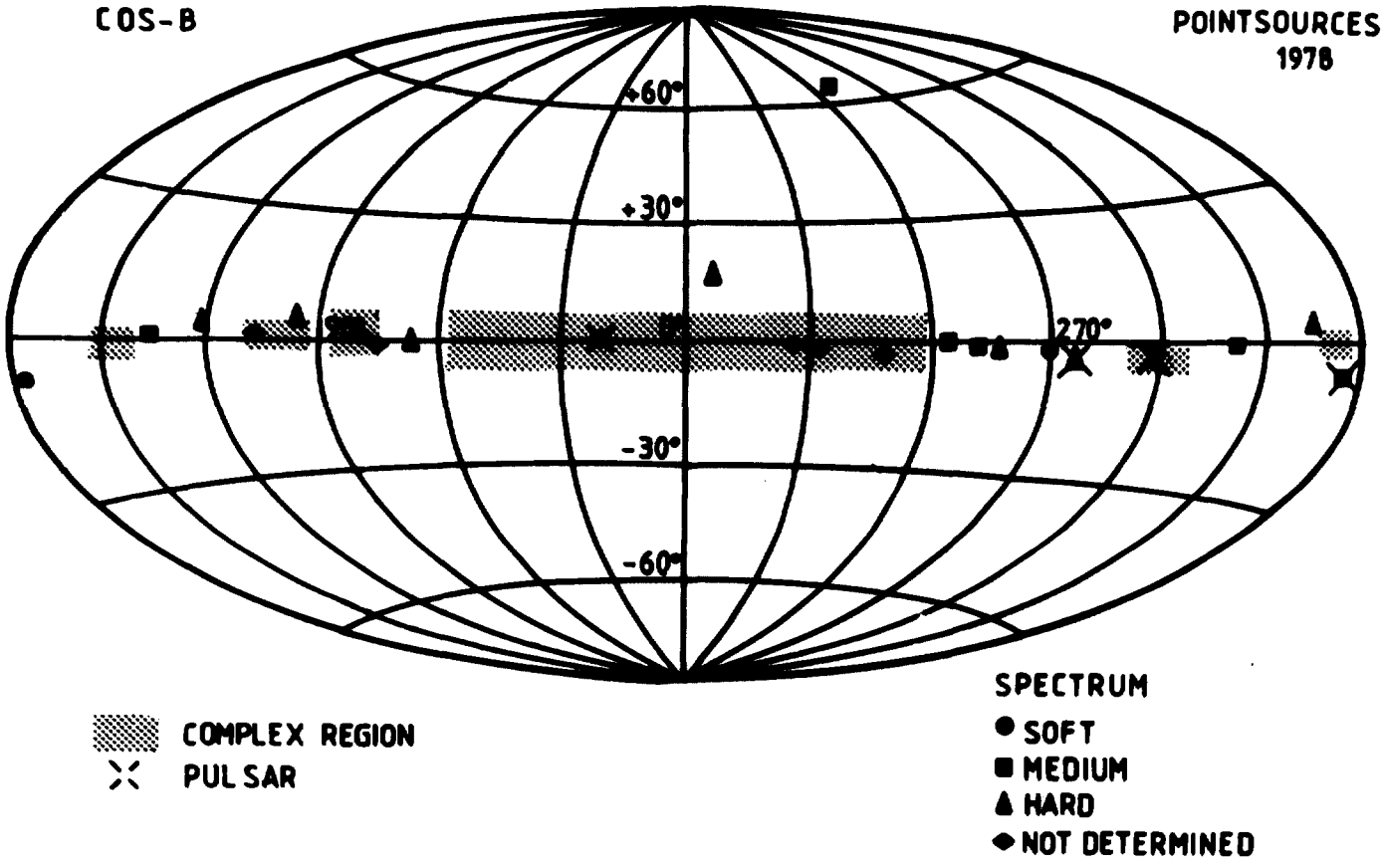
COS-B
POINTSOURCES
1978
+60°
+30°
270°
-30°
-60°
COMPLEX REGION
PULSAR
SPECTRUM
SOFT
MEDIUM
HARD
NOT DETERMINED

Figure 4

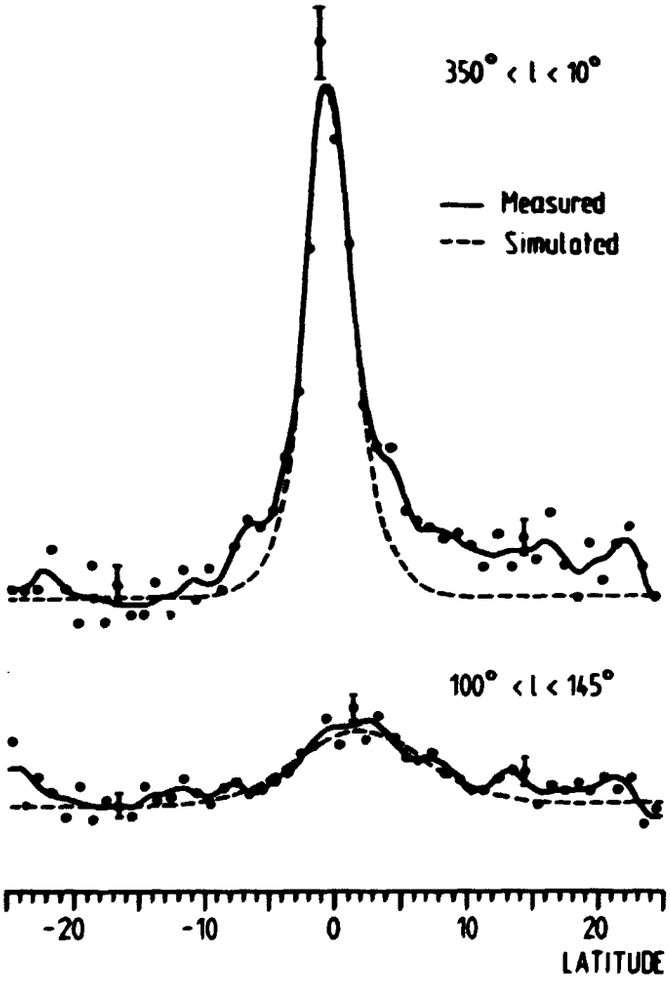
350° < l < 10°
Measured
Simulated
100° < l < 145°
-20
-10
0
10
20
LATITUDE

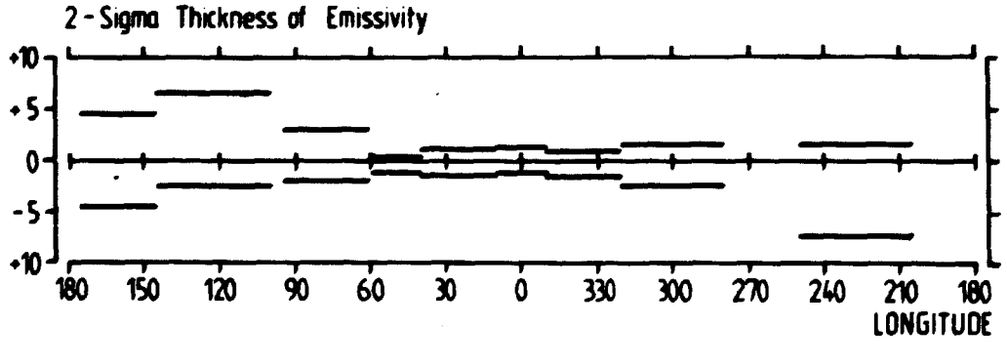
2 - Sigma Thickness of Emissivity
+10
+5
0
-5
+10
180
150
120
90
60
30
0
330
300
270
240
210
180
LONGITUDE

Figure 5